Effect of Electrolyte Diffusion on the Growth of NaCl Particles by Water Vapour Condensation

Kari E. J. Lehtinen,*,† Markku Kulmala,† Peter Ctyroky,‡ Tanja Futschek,‡ and Regina Hitzenberger‡

Department of Physical Sciences, University of Helsinki, P.O. Box 64, FIN-00014 Helsinki, Finland, and Institute for Experimental Physics, University of Vienna, Boltzmanng. 5, A-1090 Vienna, Austria

Received: January 24, 2002; In Final Form: June 17, 2002

The hygroscopic growth of NaCl particles was investigated both experimentally and theoretically. Straightforward experiments done with a humidity controlled microbalance show that a macroscopic time (hours to days) is required before the final (equilibrium) size is reached. The developed model shows that the droplets are not homogeneous salt solutions and that a finite liquid phase diffusion resistance exists. This is clearly evident from the experimental data also: the initial stage of growth shows a linear mass growth in time. This would not be possible without the liquid-phase resistance. It was also possible to determine the liquid-phase diffusion coefficient. Although the value depends on composition and temperature, the best fit with experimental data was obtained by using a value of 1.5×10^{-9} m^2/s, which agrees well with available experimental data for strong NaCl−water electrolytes.

Introduction

Atmospheric aerosol particles influence Earth's radiation balance directly by scattering and absorbing solar radiation and indirectly by acting as cloud condensation nuclei (CCN).[1] Despite the recent progress in evaluating the radiative effects of several aerosol components including sea salt and crustal material,[2−8] substantial uncertainties still remain in quantifying the source contributions for biogenic and natural emissions, of organic vapors and sea salt.[9,10] Without understanding the contribution of natural emissions to radiative forcing, we can never hope to accurately predict or understand the true effect of anthropogenic emissions.

The most recent IPCC report[8] gives large error bars for the direct aerosol effect, and even larger ones for the indirect effect. The formation of soluble aerosol particles, their water uptake under subsaturated conditions and subsequent activation as CCN are among the key questions, but processes such as nucleation, droplet activation during condensation, diffusive growth, droplet evaporation, droplet coalescence, and conversion to raindrops are very crudely taken into account in present-day atmospheric large-scale models. Because of their shortwave and longwave optical properties, clouds effectively dominate the global albedo and play a crucial role for the radiative balance of the Earth, but their microphysical properties are not included in detail in recent climate models.[7] The importance of including multicomponent aerosol populations and dynamic feedbacks in the cloud forming processes, along with the importance of coupling chemical and physical processes in predicting cloud droplet populations have been illustrated, e.g., by Kulmala et al.[11]

As marine clouds have the largest effect on the planetary albedo, the properties of marine aerosols that affect cloud droplet formation[12,13] are very important. Particularly, relatively large sea-salt particles could play a significant role in the determination of local supersaturation. NaCl is the major component in sea salt. Usually, NaCl particles are assumed to be either dry particles or homogeneous solution droplets, which correponds to the assumption that the droplets or particles are in equilibrium with the surrounding moist or dry air. CCN activation is usually described using Köhler theory, which is based on the assumption of equilibrium. If some CCN, however, are not in equilibrium because their equilibration time is too long, the predictions of Köhler theory might not apply to this aerosol. In the present study we investigate both experimentally and theoretically how rapidly large NaCl particles will achieve equilibrium with water vapor at relative humidities below 100%. In the experiments, milligrams of NaCl were used as samples.

In principle, the growth of aerosol particles under conditions of elevated relative humidity can be measured either on single particles suspended in an electrodynamic balance[14] or on-line in a tandem-DMA system.[15] The growth of bulk aerosol samples (or bulk matter in general) can be investigated using humidity-controlled microbalances, which was first done by Hänel.[16] The growth of single NaCl particles was investigated extensively some decades ago,[17,18] but at that time only equilibrium growth factors were of interest. Because of the wide-spread use of tandem DMA,[19] where particles are exposed to elevated humidities in a flow-humidifier, the equilibration time is also of interest to ensure that the particles have reached their final size before they are classified in the second DMA. Virkkula et al.[20] mentioned that at least for mixed organic/inorganic particles, the residence time in the humidified part of the tandem-DMA might not be sufficient for the particles to achieve their final size. Theoretical studies on the growth laws of aerosols under conditions of elevated humidities exist,[21] but in all these studies, the transport of water vapor is considered only in terms of gas-phase diffusion to the droplet. Water transport within the droplet or during the deliquescence process has not been published so far.

In the experimental part of the current study, the growth dynamics of salt particles (dry mass in the range 1−12 mg) are

* To whom correspondence should be addressed. E-mail: kari.lehtinen@helsinki.fi. Tel: +358-9-19150711. Fax: +358-9-19150717.
† University of Helsinki.
‡ University of Vienna.

10.1021/jp020240w CCC: $25.00
Published on Web 12/21/2002

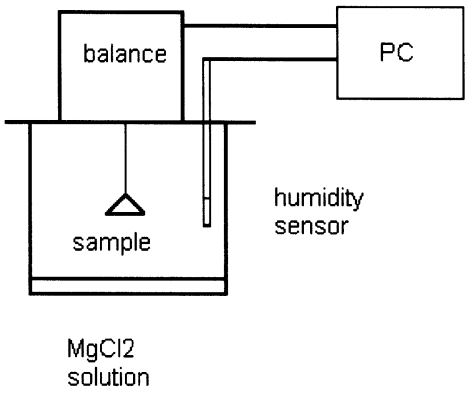

Figure 1. Schematic setup of the humidity chamber.

studied with a balance located above a humidity chamber. Different relative humidities were used to produce curves of growth as a function of time. The theoretical part includes a coupled gas-phase−liquid-phase numerical diffusion model, thus simulating both the condensation of water vapor onto the particles as well as the electrolyte diffusion within the particles. The aim was to find out how long it takes to reach equilibrium size and if the liquid-phase diffusion poses a resistance to the dynamics.

Experimental Setup

The growth curves were measured with a static humidity chamber similar to the one described by Hitzenberger et al.[22] Figure 1 shows a schematic view of the chamber. A semi-microbalance (Mettler AT 201, accuracy ±10 μg) is mounted on top of the humidity chamber. Through a sealed opening, a stainless steel tray is suspended from the balance into the chamber. The sample is put into a small (inner diameter 13 mm) plastic dish and placed on the tray. Humidity in the chamber is controlled by using aqueous solutions of $MgCl_2 \cdot 6H_2O$ of different concentrations. Changes to the design of the chamber enabled adding water or salt to this solution without opening the chamber, so deliquescence and efflorescence curves can be obtained if needed. Figure 2 gives the curve of relative humidity vs concentration of the $MgCl_2$ solution (data based on Low[23]). The crystal water has to be taken into account in the calculations of the amount of salt needed to obtain a specified humidity. In principle, the maximum humidity in the chamber should be 100% (obtained with pure water as humidity controlling "solution"). A narrow opening along the shaft of the balance, however, could not be sealed totally without obstructing the weighing process, so some losses of water vapor could not be prevented. The actual relative humidity in the chamber was therefore measured with a Vaisala HMP35 probe, which also gives temperature data. This probe was calibrated using saturated solutions of K_2SO_4 (94% relative humidity at 20 °C) and LiCl (11% relative humidity at 20 °C). According to factory specification, such a calibration ensures an accuracy of better than 2% relative humidity. The temporal trends of humidity, temperature and sample mass were recorded with a computer.

To check the long-term stability of the balance including weighing tray and dish at elevated humidity, tests were performed with pure water as humidity controlling "solution". The long-term stability of the microbalance with the weighing tray and the plastic dish at high relative humidity (90%) was found to be ±0.3 mg (testing period: 3.5 days). As the NaCl sample masses (1−12 mg) increased by factors of 5 to >20, this long-term stability was found to be sufficient.

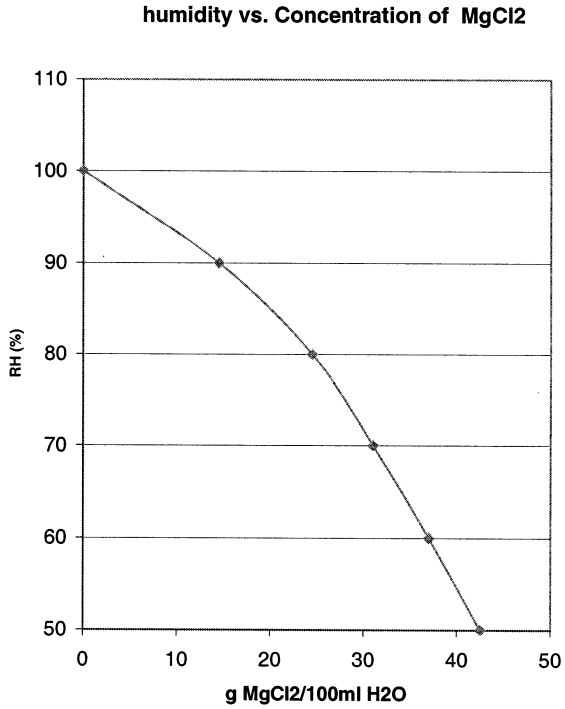

Figure 2. Relative humidity vs concentration of $MgCl_2$ solution. The crystal water associated with $MgCl_2 \cdot 6H_2O$ has to be taken into account separately. Original curve given by Low.[22]

Theory

The salt particle deliquescence evolves in the following way. The initial stage of condensation results in a thin layer of saltwater solution, having a salt mole fraction x_s of 0.0995. This value corresponds to the maximum solubility of NaCl salt in water at 25 °C.[24] Now, if the diffusion processes inside the particle would be infinitely fast, this would be the case during the whole dissolution of salt, i.e., as soon as water has condensed onto the particle, salt would dissolve immediately and the particle would be a saturated salt solution droplet. However, if the liquid phase diffusion is not fast enough, a concentration profile will form in the solution with a highly concentrated solution at the surface of the solid salt core and a less concentrated solution at the surface of the droplet, which in turn will lower the condensation rate. This is what we believe will happen in this case.

Water activity in the solution droplet a_w, as a function of mole fraction x_w can be estimated by

$$a_w = -8.8672 + 18.085x_w - 8.2188x_w^2 \qquad (1)$$

which is a least-squares best second-order polynomial fit to the experimental data of Robinson and Stokes.[25] The fit and the experimental points are compared in Figure 3.

The vapor molar concentration of water $c_{w,surf}$ just above the particle surface is

$$c_{w,surf} = a_w c_{sat} \qquad (2)$$

in which the activity a_w must be calculated using the water mole fraction right below the particle surface. The saturation water vapor concentration c_{sat} corresponds to the case in which no salt is present. In equilibrium, the vapor concentration at the surface is equal to the value far from the particle. Thus at equilibrium we must have

$$a_w = S \qquad (3)$$

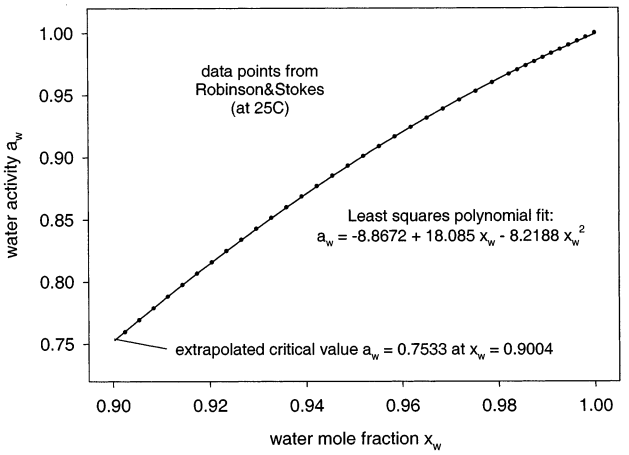

Figure 3. Water activity as a function of water mole fraction (in solution) at 25 °C.

in which S is the saturation ratio. The second-order polynomial expression in eq 1 enables an analytical solution of the equilibrium water mole fraction (in solution) as a function of the saturation ratio. Furthermore, this can be transformed trivially into growth factor GRF, i.e., ratio of equilibrium droplet mass to initial salt particle mass:

$$\mathrm{GRF} = 1 + \frac{M_w}{M_s}\left(\frac{x_w}{1 - x_w}\right) \tag{4}$$

In eq 4, M_w and M_s are the molecular weights and x_w is the mole fraction of water, respectively. Because in this study we are following the growth of particles as a function of time, we can thus also get information concerning this equation that concerns the approach to equilibrium.

The salt particle is approximated with a half-sphere geometry, as well as assuming spherical symmetry for the transport processes. Essentially, we are then solving for the whole sphere, but dividing by 2 for the mass growth rates.

The diffusion of water and salt in the solution phase are governed by the spherically symmetric binary diffusion equations:[26]

$$\frac{\partial c_w}{\partial t} + \nabla(c_w v^*) = \nabla(cD_{ws}\nabla x_w) \tag{5a}$$

$$\frac{\partial c_s}{\partial t} + \nabla(c_s v^*) = \nabla(cD_{ws}\nabla x_s) \tag{5b}$$

in which c_w and c_s are the molar concentrations of water and salt, respectively. The total molar concentration of the solution is c, and the mole fractions of water and salt are x_w and x_s, respectively. D_{ws} is the binary diffusion coefficient of salt and water and v^* the molar average velocity ($v^* = x_s v_s + x_w v_w$) of the components. Equations are equivalent, and only one of them (in this case eq 5a) needs to be solved.

In the gas phase the equation for water vapor transport is of similar form:

$$\frac{\partial c_w^{\,g}}{\partial t} + \nabla(c_w^{\,g} v^*) = \nabla(c^g D_{wg}\nabla x_w^{\,g}) \tag{6}$$

Typically, a detailed solution for the gas phase is not necessary. This is because the molar concentration of vapor in the gas phase retains its functional form and the changes in conditions result only in changing boundary conditions (pseudo-steady-state assumption; see, e.g., Wagner[27]). This method is employed here, resulting in the following molar flux of water onto the droplet of radius r_p:

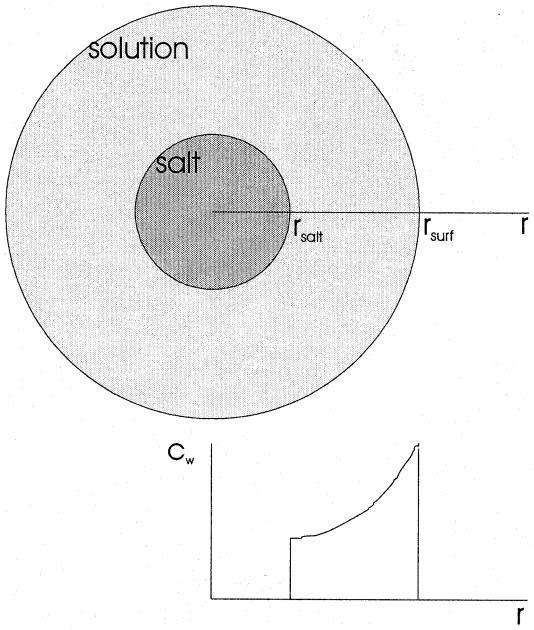

Figure 4. Deliquescence of salt particle: initial stage. All salt has not dissolved yet, and the salt core of the particle is surrounded by a layer of strong electrolyte solution. The bottom graph shows the water molar concentration qualitatively as a function of radial position.

$$N_{w,surf} = 4\pi r_p D_{wg}(c_{w,\infty}^{\,g} - c_{w,surf}^{\,g}) \tag{7}$$

Here $c_{w,\infty}^{\,g}$ is the molar concentration of water vapor far away from the droplet, and $c_{w,surf}^{\,g}$ is that at the surface. The surface molar concentration is obtained from the boundary condition at the solution−gas interface (see Figure 4):

$$\lim_{r \to r_{surf}}[cD_{ws}\nabla x_w] = 4\pi r_p D_{wg}(c_{w,\infty}^{\,g} - c_{w,surf}^{\,g}) \tag{8}$$

This just means that the amount of water flux is continuous across the interface. However, there is additional complexity in this case, because of the fact that the condensing water increases the size of the particle. Thus the location for the boundary condition changes with time. We effectively avoid this problem by choosing a moving coordinate system.

The other boundary condition, at the surface of the salt core, is

$$x_w = 0.9005 \qquad \text{at} \qquad r = r_{salt} \tag{9a}$$

corresponding to maximum solubility. When all the salt has dissolved, this is replaced by

$$\nabla x_w = 0 \qquad \text{at} \qquad r = 0 \tag{9b}$$

In the numerical scheme we initially assume a very thin solution layer surrounding the salt core, one thousandth of the salt particle in volume. This layer is initially divided in three shells, with each having the same amount of salt. Then the water starts condensing into the outermost layer from the gas phase, and subsequently diffusing deeper into the solution layer. When the water reaches the innermost shell (on top of the salt-core), more salt will dissolve. The mole fraction of salt in the innermost shell will be always kept constant at 0.0995. Three shells are of course not enough to resolve this problem accurately enough.

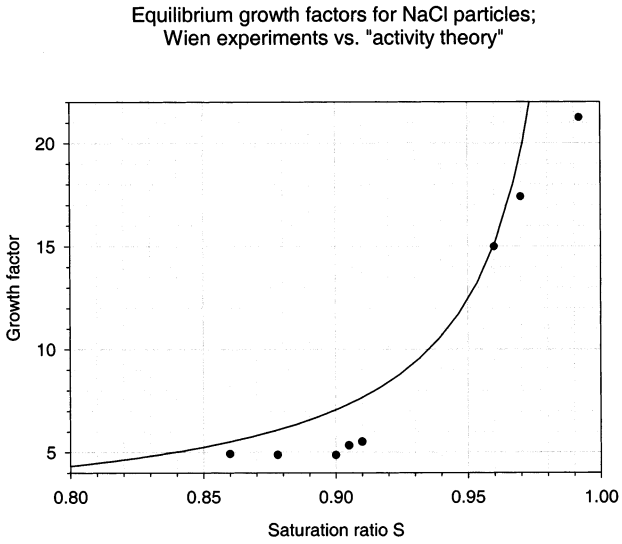

Figure 5. Growth factor vs saturation ratio at equilibrium. The points represent experimental growth factors; the solid line, theory.

Thus we have adopted a shell splitting routine, in which a shell is divided in two equal parts (in terms of salt content) every time its volume becomes larger than 2 times that of a neighboring shell. This condition will affect only the innermost and outermost shells. The innermost shell will grow because of more salt dissolving into it and the outermost shell because of water condensation. The volumes of the other shells stay roughly the same during the dissolution of the core.

For the diffusion coefficients, we used $D_{wg} = 2.6 \times 10^{-5}$ m^2/s for diffusion of water vapor in air[28] (at $T = 25$ °C) and $D_{ws} = 1.5 \times 10^{-9}$ m^2/s for diffusion of water in the strong electrolyte solution.[29] The electrolyte diffusion coefficient is a weak function of concentration, varying in the range 1.47×10^{-9} to 1.6×10^{-9} m^2/s, depending on the molality. Thus it is reasonable to use a constant value.

The results were checked in terms of grid resolution by using more shells. We found out that the discretization routine described above seems to be sufficient to resolve the growth rate of the particle within three significant figures.

Results and Discussion

From theory, it is straightforward to compute the equilibrium size, i.e., the growth factor that would be obtained if the same conditions could be applied for an infinite time. These results are summarized in Figure 5. The points represent experimental results from different conditions, the solid line an ideal curve from theory (eqs 1, 3, and 4), relating the growth factor to the saturation ratio. It seems that the experimental trend follows theory qualitatively quite nicely, but also some discrepancies are evident. From these points we select the ones that agree better with theory for closer inspection.

In Figure 6, the experimental growth data are compared with model results for the cases (a) $m = 1$ mg and $S = 0.87$, (b) $m = 6$ mg and $S = 0.96$, and (c) $m = 3$ mg and $S = 0.97$. Two modeling approaches are compared: one assuming instantaneous mixing by diffusion in the liquid phase, the other having a detailed numerical solution to the diffusion equation in the solution also. The instantaneous diffusion model means that only condensation from the gas phase to the liquid phase is considered, naturally also updating the liquid-phase concentration all the time.

In the pure condensation model, the condensation rate increases with particle size, as is seen in eq 7. This is also clearly

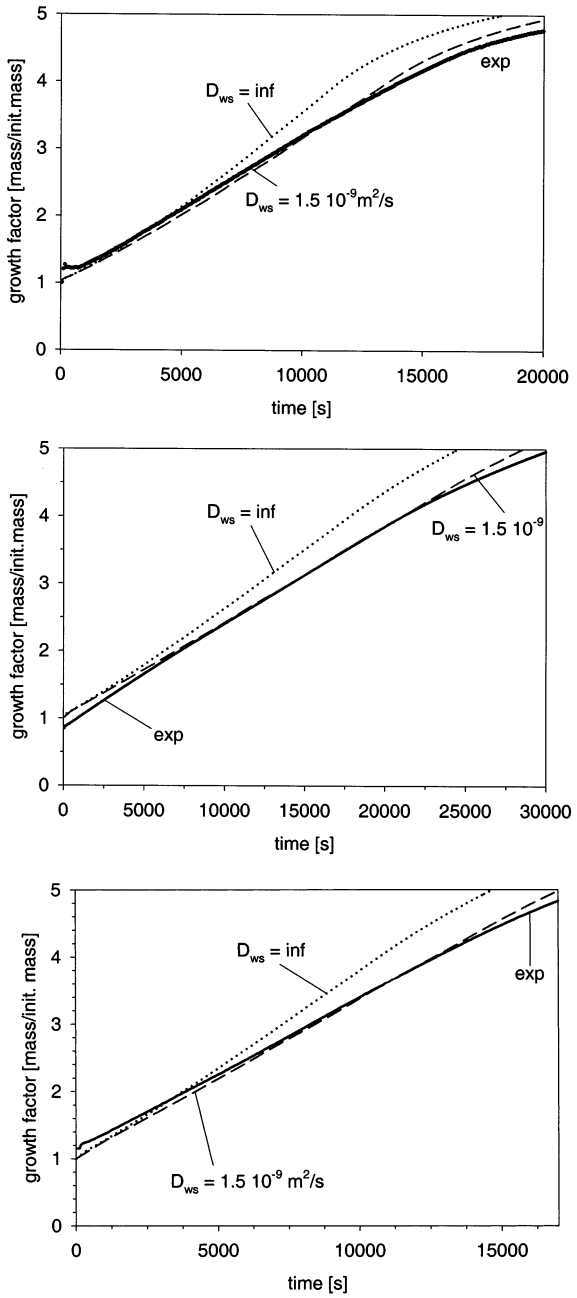

Figure 6. Growth of (a) a 1 mg NaCl particle in 87% relative humidity, (b) a 6 mg NaCl particle in 96% relative humidity, and (c) a 3 mg NaCl particle in 97% relative humidity. The solid line is the experimental result. The dotted line ($D_{ws} = \infty$) is the result of a simulation assuming instantaneous diffusional mixing in the solution. The dashed line is the result when diffusion in the solution is also considered.

evident in the results presented in Figure 5. However, the experimental growth curves show an almost linear growth pattern while salt is still dissolving. This linear initial mass growth of the particles is a clear indication that the diffusion in the solution layer is slowing down particle growth. Furthermore, the model assuming no diffusional resistance seems to overpredict the growth rate significantly.

In all cases (Figures 6a−c) the model combining condensation and solution phase diffusion seems to describe the growth observed in experiments very well. At the initial stage, when a salt core is still present, the agreement is nearly perfect.

The model has also been scaled down to particle sizes of more practical (atmospheric) interest; i.e., the simulations have

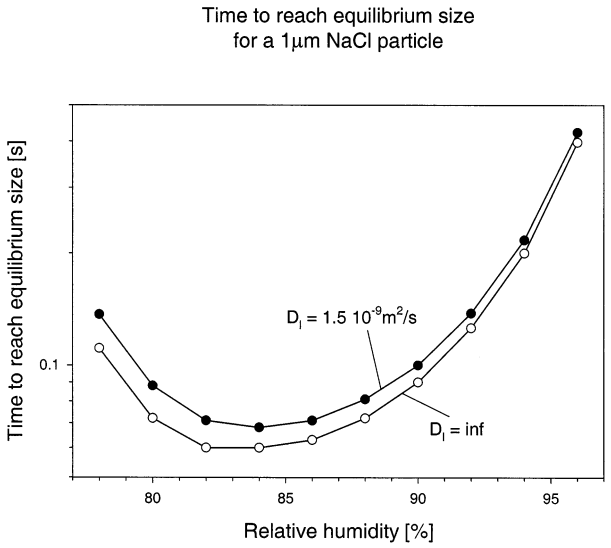

Figure 7. Time to reach equilibrium size for a NaCl particle of diameter 1 μm, as a fuction of relative humidity.

been done for a particle of initially 1 μm in diameter. In Figure 7 the time to reach the equilibrium size, defined in this case as 95% of the equilibrium size in mass, is plotted as a function of relative humidity. The calculations were done both for instantaneous solution phase diffusion ($D_{ws} = \infty$, open circles) and for a finite value of $D_{ws} = 1.5 \times 10^{-9}$ m^2/s (solid circles) for the diffusion coefficient. It seems clear that taking into account solution phase diffusion has a clear effect on the results, especially for the low relative humidities, for which the effect can be roughly 20% in terms of growth time to equilibrium.

One important result of this study is that the deliquescence process from a dry salt particle to equilibrium size is a finite process and not instantaneous, as practically assumed when using the Köhler expression.[28] The growth time is of the order of 0.1s for a 1 μm particle and has a d_p^2 size dependence, which means that growth of a 10 μm particle lasts roughly 10 s. Another interesting feature of Figure 7 is the minimum in the growth time. This is because the competition of two things affecting the growth time: the higher mass transfer (and thus decreasing growth time) rate caused by the higher relative humidity and the larger equilibrium size (and thus increasing growth time).

One aspect neglected in these studies was the possible role of other transport mechanisms than diffusion. E.g., the gravitational fall of droplets can induce internal flows that affect transport. In this study, such effects were neglected to coincide with the experiments.

Conclusions

The hygroscopic growth of milligram size NaCl particles was investigated experimentally and theoretically. The results obtained show a time lag before the equilibrium size is achieved. For relevant sizes in atmospheric point of view the equilibrium sizes are reached within 10 s (for 10 μm particles) and 0.1 s (for 1 μm particles). The droplet evolves with time from a partially dissolved salt core surrounded by an inhomogeneous solution film to a homogeneous droplet in equilibrium with the surrounding vapor.

The experimental growth data show initially an almost perfectly linear mass growth rate in time, as long as there still is undissolved salt in the particle core. This contradicts the assumption of an internally homogeneous solution droplet, for which the solution phase diffusion would be infinitely fast, because in that case, the growth would be a pure condensation process and the mass flux should increase with size. It is clearly seen that there is a concentration gradient within the droplet, which exists not only during incomplete dissolution, but all the way until equilibrium with the surrounding vapor is reached.

The numerical model runs, in which both gas phase and liquid phase diffusion are considered, support this conclusion. Furthermore, the modeled time evolution of the growth factor (mass/init. mass) follows the experimental data reasonably well for most of the cases studied, when a constant value 1.5×10^{-9} m^2/s is selected for the solution phase diffusion coefficient. The value of the diffusion coefficient, reported by Lobo[29] is a weak function of molality of the solution and varies between 1.473×10^{-9} and 1.594×10^{-9} m^2/s. Thus, our value of choice agrees well with experimentally obtained data.

Acknowledgment. The experimental work was part of the EUROTRAC-II subproject AEROSOL and funded in part by a grant from the Hochschuljubiläumstiftung der Stadt Wien, H180/99. The development of the prototype of the humdity chamber was funded by the Austrian Science Fund. The support by the Academy of Finland (project number 400207) is also acknowledged.

References and Notes

(1) Charlson, R. J.; Schwartz, S. E.; Hales, J. M.; Cess, R. D.; Coakley, J. A.; Hansen, J. E.; Hofmann, D. J. *Science* **1992**, *255*, 423.

(2) Chuang, C. C.; Penner, J. E.; Taylor, K. E.; Grossman, A. S.; Walton, J. J. *J. Geophys. Res*. **1997**, *102*, 3761.

(3) Haywood, J. M.; Ramaswamy, V. *J. Geophys. Res*. **1998**, *103*, 6043.

(4) Kaufman, Y. J.; Fraser, R. S. *Science* **1997**, *277*, 1636.

(5) Winter, B.; Chylek, P. *Tellus* **1997**, *49B*, 72.

(6) Sokolik, I. N.; Toon, O. B. *Nature* **1996**, *381*, 681.

(7) Haywood, J.; Boucher, O. *Rev. Geophys.* **2000**, *38*, 513.

(8) IPCC: Climate Change 2001: The Scientific Basis. Contribution of Working Group I to the Third Assessment Report of the Intergovernmental Panel on Climate Change, Houghton.

(9) Jacobson, M. Z.; Hansson, H. C.; Noone, K. J.; Charlson, R. J. *Rev. Geophys.* **2000**, *38*, 267.

(10) Jacobson, M. Z. *J. Geophys. Res.* **2001**, *106 D1*, 1551.

(11) Kulmala, M.; Laaksonen, A.; Korhonen, P.; Vesala, T.; Ahonen, T.; Barrett, J. C. *J. Geophys. Res.* **1993,** *98*, 22949.

(12) Fitzgerald, J. W. *Atmos. Environ.* **1991**, *25A*, 533.

(13) O'Dowd, C. D.; Smith, M. H.; Consterdine, I. E.; Lowe, J. A. *Atmos. Environ.* **1997**, *31*, 73.

(14) Rubel, G. O. In *Aerosol Chemical Processes in the Environment*; Spurny K. R., Ed.; Lewis Publishers: Boca Raton, FL, 2000; p 197.

(15) Hämeri, K.; Väkevä, M.; Aalto, P. P.; Kulmala, M.; Swietlicki, E.; Zhou, J.; Seidl, W.; Becker, E.; Dowd, C. O. *Tellus* **2001**, *53B*, 359.

(16) Hänel, G. *Adv. Geophys.* **1976**, *19*, 74.

(17) Tang, I. N. *J. Aerosol Sci.* **1976**, *7*, 361.

(18) Tang, I. N.; Munkelwitz, H. R. *Atmos. Environ.* **1993**, *27A*, 467.

(19) Rader, D. J.; McMurry, P. H. *J. Aerosol Sci.* **1986**, *17*, 771.

(20) Virkkula, A.; vanDingenen, R.; Raes, F.; Hjorth, J. *J. Geophys. Res* **1999**, *104*, 3569.

(21) Kerminen, V. M.; Wexler, A. S. *Atmos. Environ*. **1995**, *29*, 3263.

(22) Hitzenberger R.; Dusek U.; Berner A.; Alabashi, *Aerosol Sci. Technol*. **1997**, *27*, 116.

(23) Low, R. D. H. *J. Rech. Atmos*. **1969**, *4*, 65.

(24) *CRC Handbook of Chemistry and Physics*; CRC Press: Boca Raton, FL, 2000.

(25) Robinson, R. A.; Stokes, R. H. *Electrolyte Solutions*. Butterworth: London, 1959.

(26) Bird R. B.; Stewart W. E.; Lightfoot, E. N. *Transport Phenomena*; Wiley: New York, 1960.

(27) Wagner, P. E. Aerosol growth by condensation. In *Aerosol Microphysics II: Chemical Physics of Microparticles*; Marlow, W. H., Ed.; Springer: Berlin, 1982.

(28) Rogers R. R.; Yau M. K. *A Short Course in Cloud Physics*; Pergamon Press: Oxford, U.K., 1991.

(29) Lobo V. M. M. *Electrolyte Solutions: Literature Data on Thermodynamic and Transport Properties*; University of Coimbra Press: Coimbra, Portugal, 1984.